

Electronic Supplementary Information for:

**Interaction of Beta-Lactoglobulin and Bovine Serum Albumin with Iron Oxide (α -Fe₂O₃)
Nanoparticles in the Presence and Absence of Pre-Adsorbed Phosphate**

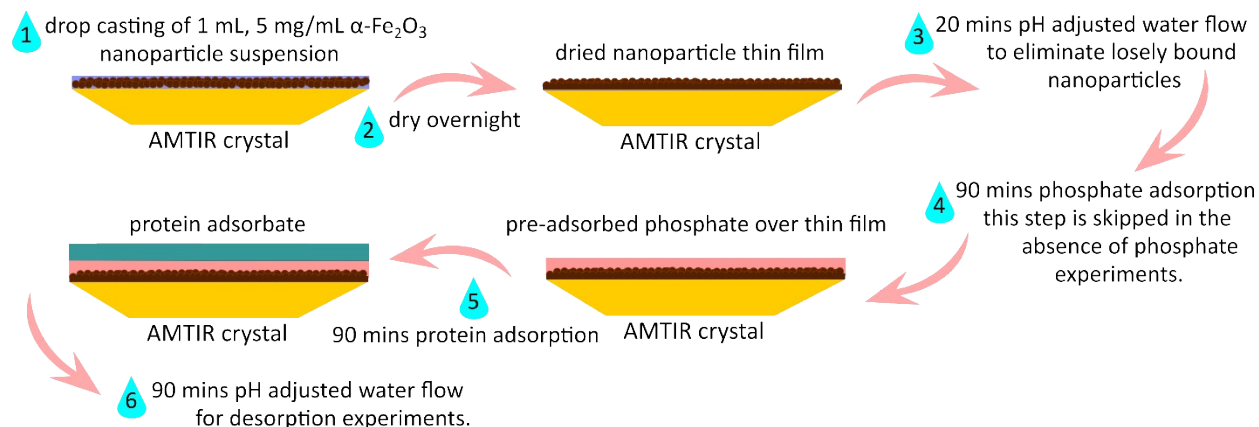
Irem B. Ustunol,^a Elizabeth K. Coward,^b Eleanor Quirk,^a and Vicki H. Grassian^{a,b,*}

^a Department of Nanoengineering, ^b Department of Chemistry and Biochemistry,

University of California, San Diego, La Jolla, CA, 92093

The supplementary material contains 1 scheme, 6 figures, 1 table, and 6 pages in total.

* Corresponding author at University of California, San Diego, La Jolla, CA, 92093, USA. *Tel:* +1 858-534-2499, *E-mail address:* vhgrassian@ucsd.edu. ORCID : 0000-0001-5052-0045 (Vicki H. Grassian), 0000-0003-0370-118X (Irem B. Ustunol), 0000-0001-9959-1266 (Eleanor Quirk), 0000-0002-3279-8788 (Elizabeth K. Coward).



Scheme S1. A detailed schematic of the ATR-FTIR protein adsorption and desorption experimental steps.

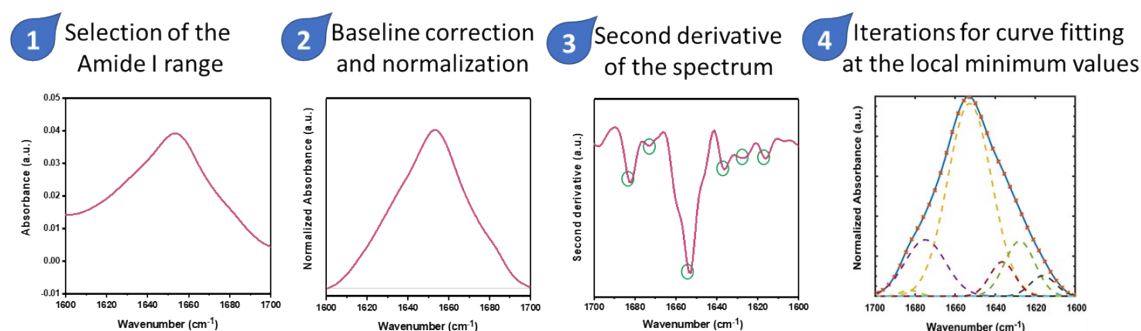


Figure S1. Curve fitting approach applied to the amide I band of kinetic protein ATR-FTIR spectra. (1) The amide I band range (1600 to 1700 cm^{-1}) from the raw data of each adsorbed protein was extracted at a selected reaction time. (2) This range was baseline corrected to a linear-line and normalized to the amide I band range with the highest observed peak intensity. (3) The second derivatives of the spectra were processed, and the local minimum values were used to identify the band position of each secondary component. (4) The amide I band was deconvoluted into Gaussian curves, to achieve the best composite results.

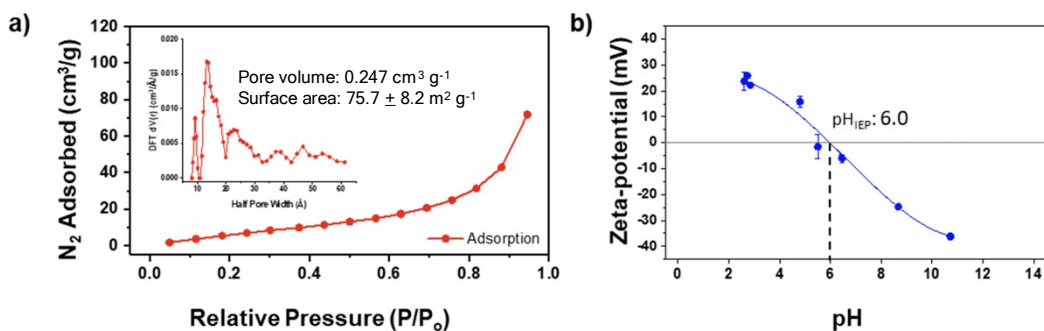


Figure S2. (a) BET isotherm of N_2 adsorption and Density Functional Theory (DFT) pore size distribution for $\alpha\text{-Fe}_2\text{O}_3$ nanoparticles and (b) zeta-potential measurements of $\alpha\text{-Fe}_2\text{O}_3$ nanoparticles in 10 mM NaCl as a function of pH. The isoelectric point (pH_{IEP}) of nanoparticles was determined to be approximately 6.

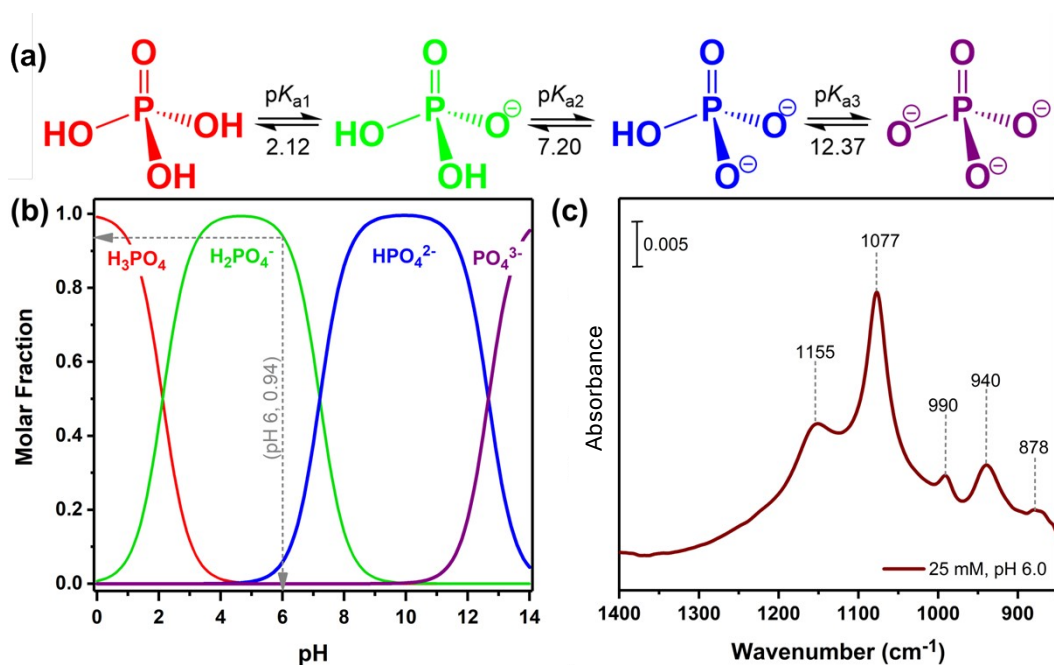


Figure S3. (a) Phosphate acid-base reaction equilibria where $\text{p}K_{\text{a}1} = 2.12$, $\text{p}K_{\text{a}2} = 7.20$, and $\text{p}K_{\text{a}3} = 12.37$; (b) phosphate speciation diagram calculated using Henderson-Hasselbalch equation shows that 0.94 molar fraction of phosphate speciation at pH 6 is H_2PO_4^- . (c) ATR-FTIR spectrum of aqueous phase phosphate (25 mM) in 10 mM NaCl solution at pH 6.

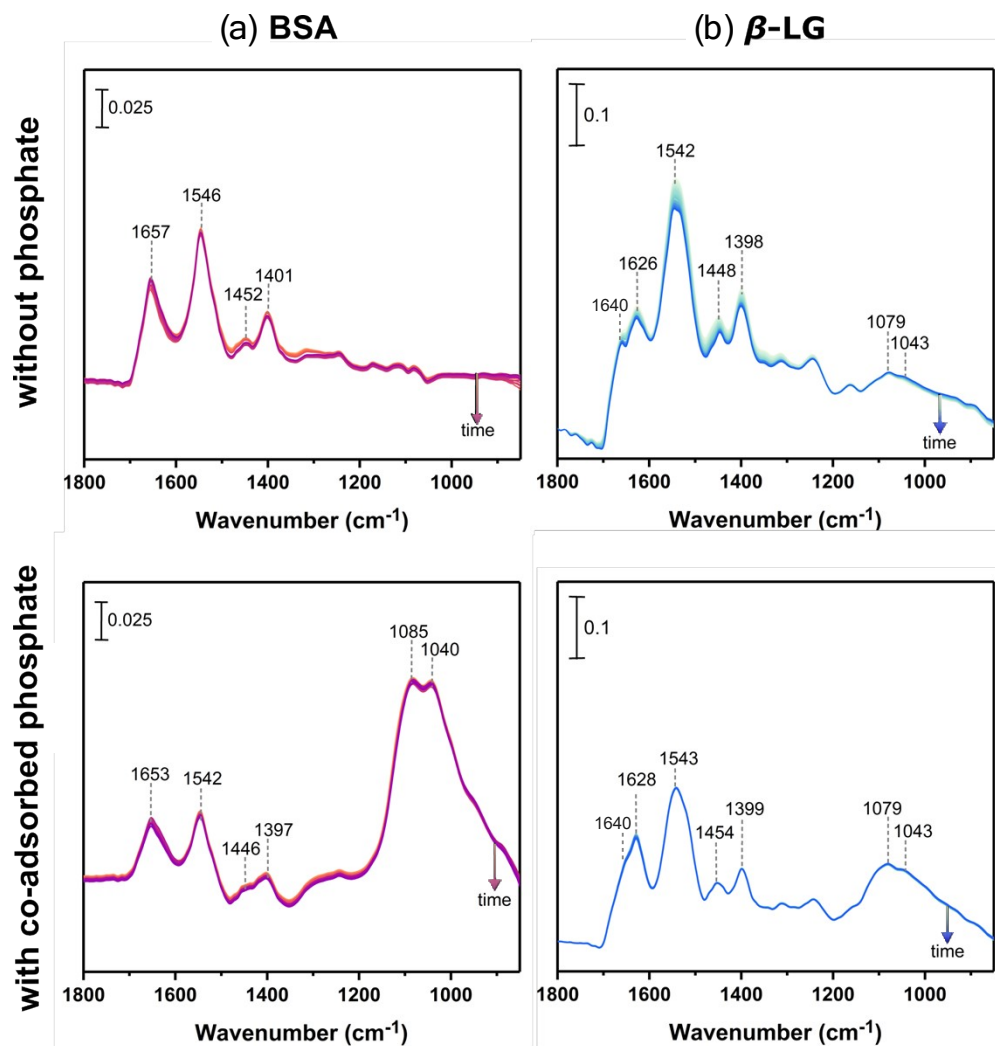


Figure S4. ATR-FTIR spectra of (a) BSA and (b) β -LG during desorption from α - Fe_2O_3 with 10 mM NaCl, in the presence (top) and absence (bottom) of co-adsorbed phosphate. Scale bars indicate absorbance, and colorscale denotes the time each spectrum was collected during desorption.

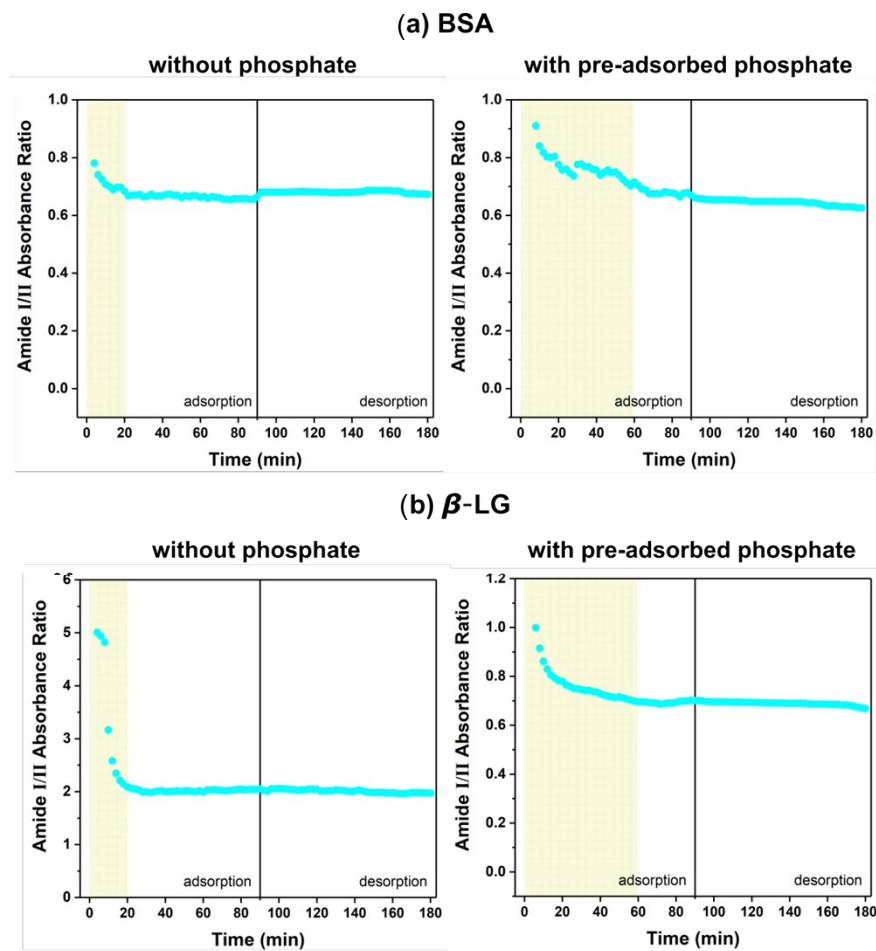


Figure S5. Amide I and II peak absorbance intensities of BSA and β -LG during adsorption onto α -Fe₂O₃ nanoparticles (0-90 min) and desorption (90-180 min).

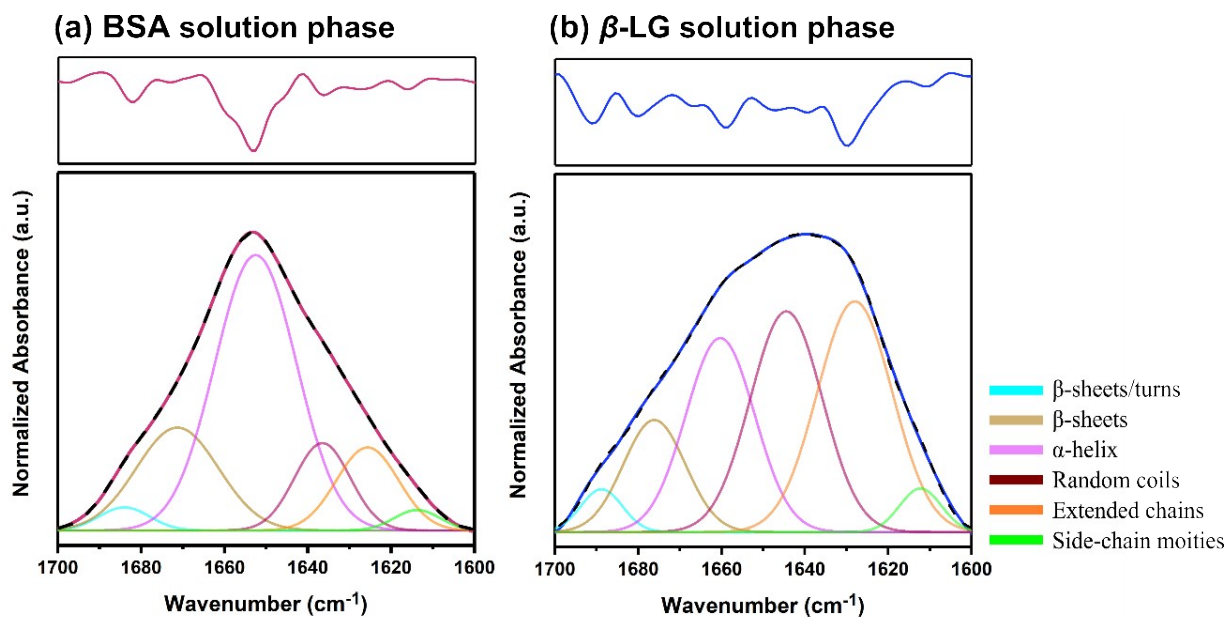


Figure S6. Background subtracted and normalized protein amide I band for secondary structural analysis with curve fitting results for (a) BSA and (b) β -LG solutions at pH 6.0.

Table S1. Summarized vibrational frequencies (cm^{-1}) of peak centers associated with individual secondary structure components of BSA and β -LG after curve fitting.

	Secondary structure	Solution phase (cm^{-1})	Adsorbed on α - Fe_2O_3 (cm^{-1})		Adsorbed on phosphate-coated α - Fe_2O_3 (cm^{-1})	
			4 min	90 min	4 min	90 min
BSA	β -sheets	1684	1690	1690	1689	1683
	Turns	1671	1677	1677	1674	1671
	α -helices	1652	1659	1658	1658	1655
	Random coils	1636	1643	1645	1644	1642
	Extended chains	1625	1629	1631	1631	1630
	Side-chain moieties	1613	1612	1612	1612	1611
	Secondary structure	Solution phase (cm^{-1})	4 min	90 min	4 min	90 min
β -LG	β -sheets	1688	1695	1690	1691	1688
	Turns	1676	1676	1680	1683	1679
	α -helices	1660	1658	1658	1666	1661
	Random coils	1644	1650	1643	1647	1644
	Extended chains	1628	1635	1628	1629	1626
	Side-chain moieties	1612	1618	1612	1614	1611